



Automatic Measurement of Silicon Lattice Spacings in High-Resolution Transmission Electron Microscopy Images Through 2D Discrete Fourier Transform and Inverse Discrete Fourier Transform

Fang Wang¹ · Yushu Shi¹ · Shu Zhang¹ · Xixi Yu^{1,2} · Wei Li¹

Received: 14 September 2021 / Revised: 25 January 2022 / Accepted: 28 January 2022 / Published online: 6 April 2022
© The Author(s) 2022

Abstract

Line width (i.e., critical dimension, CD) is a crucial parameter in integrated circuits. To accurately control the CD in manufacturing, a reasonable CD measurement algorithm is required. We develop an automatic and accurate method based on a two-dimensional discrete Fourier transform for measuring the lattice spacings from high-resolution transmission electron microscopy images. Through the two-dimensional inverse discrete Fourier transform of the central spot and a pair of symmetrical diffraction spots, an image containing only a set of lattice spacings is obtained. Then, the pixel span of the lattice spacing is calculated through the centre of gravity method. Finally, we estimate the standard CD value according to the half-intensity method. The silicon crystal lattice constant guarantees the accuracy and traceability of the CD value. Through experiments, we demonstrate the efficiency of the proposed method, which can be conveniently applied to accurately measure CDs in practical applications.

Keywords Transmission electron microscopy · Line width · Crystal lattice constant · Traceability

1 Introduction

The nano line width (i.e., critical dimension, CD) is a crucial parameter in integrated circuits. With continuous reduction of the line feature size, requirements for measurement accuracy continue to increase. As described in the International Technology Roadmap for Semiconductors, the measurement uncertainty of the physical CD needs to be reduced to 0.7 nm by 2024 [1, 2].

Currently, numerous techniques have been developed for CD measurement, including atomic force microscopy (AFM), scanning electron microscopy (SEM), and transmission electron microscopy (TEM). AFM can generate three-dimensional line width images with near-atomic spatial resolution [3–5]. The image is the convolution result between the actual surface topography and the tip geometry used during scanning [6, 7]. However, it is difficult to accurately estimate

the tip geometry because the tip wears during AFM scanning [8]. Consequently, it is difficult to reconstruct the true shape of a specimen from a distorted image via morphological operations of dilation and erosion.

SEM is also widely applied for CD measurement owing to its high resolution and efficiency [9–11]. After the image is obtained, an appropriate algorithm is needed to extract the line features from the intensity profile. The model-based library for CD determination, which was written as an international standard (ISO/DIS 21466.1) in 2019, is a mainstream method [12]. This method, which is based on Monte Carlo simulation, generates a set of simulated secondary electron lines according to the designed input parameters. After acquiring an SEM image, one should identify the best fit between the measured and simulated lines. The CD values can be obtained within the range of the library data. However, for each sample material and CD value, a corresponding library needs to be produced, which is a huge project and inflexible in the actual measurement. The existing model-based library in our laboratory is only suitable for Au-based CD structures and CD values exceeding 200 nm.

TEM is a distinguished CD measurement method. It became recognized especially after the incorporation of the Si {220} lattice parameter ($d_{220} = 192.0155714 \times 10^{-12}$ m,

✉ Yushu Shi
shiys@nim.ac.cn

¹ National Institute of Metrology, Beijing 100029, China

² Shenzhen Institute for Technology Innovation, National Institute of Metrology, Shenzhen 518038, China

$u_c = 0.0000032 \times 10^{-12}$ m) into the Mise en Pratique at the 2018 meeting of the Consultative Committee for Length [13, 14]. If the CD sample contains monocrystalline silicon, the line features and periodical silicon crystal lattice spacings can be visible in an image acquired via high-resolution transmission electron microscopy (HRTEM) or scanning transmission electron microscopy (STEM) [15, 16]. We can use the lattice spacings in the image as a ruler to directly measure the line width. The measurement principle is detailed in [17, 18]:

1. The CD value of the internal CD structure made of monocrystalline silicon is equal to the number of lattice spacings multiplied by the lattice constant; that is, $W = d \times N$, where W is the CD value, d is the lattice constant, and N is the number of lattice spacings within the CD structure (Fig. 1a). In addition, the thickness of amorphous layers around the structure needs to be considered in the measurement.
2. Otherwise, the CD needs to be calculated from the lattice constant and the pixel spans of the lattice spacings and line width; that is $W = d \times N_w / N_d$, where N_d denotes the pixel span of each lattice spacing, and N_w denotes the pixel span of the CD structure (Fig. 1b).

The CD value can be traced to the meter definition of the international system of units (SI) via the lattice constant since the value is a secondary realization of the meter. The measurement accuracy can reach the atomic level. Using this method, Takamasu et al. [19, 20] measured the line width with sub-nanometer accuracy and proposed a line edge detection method based on STEM images. The expanded

uncertainty was less than 0.3 nm for a line width of 50 nm. In 2017, the Physikalisch-Technische Bundesanstalt (PTB) and the National Institute of Standards and Technology (NIST) compared the IVPS10-PTB standards with nominal CDs of 50 nm, 70 nm, 90 nm, 110 nm, and 130 nm. The measurement results showed that the deviations were between -1.5 nm and 0.3 nm [21]. The National Institute of Metrology in China is also studying nano-geometric metrology based on the silicon lattice parameter. With the successful application of the Si {220} lattice parameter in the CD measurement of integrated circuits, the measurement technique has attracted increasing attention from research institutions. Although the basic measurement principle has been verified by domestic and foreign researchers, several factors affecting the measurement results need to be addressed.

According to the measurement principle, the measurement of lattice spacings is critical for the accuracy of CD values. Generally, the lattice spacings are manually measured using the TEM integrated software DigitalMicrograph (Fig. 2: an HRTEM image of Si acquired at a magnification of 790 k with 2048×2048 pixels). First, we drew a rectangular frame perpendicular to the measured lattice spacings on the TEM image. The corresponding profile in the rectangular frame was displayed in a pop-up window. Then, we moved the left and right sides of the dotted box in the pop-up window to the center of the lattice stripes. The distance between the left and right sides of the dotted box was displayed automatically. The measured lattice constant was equal to the distance divided by the number of lattice spacings contained in the dotted box.

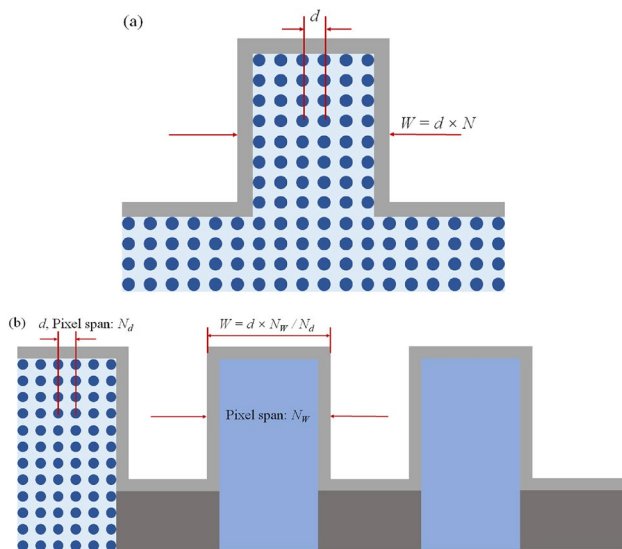


Fig. 1 TEM-based CD measurement principle for monocrystalline silicon **a** within the CD structure and **b** outside the CD structure

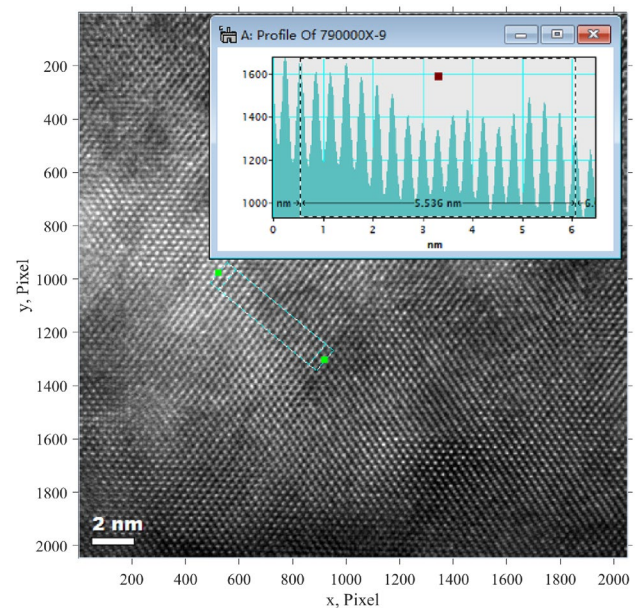


Fig. 2 Lattice spacing measurement with DigitalMicrograph

Numerous researchers have utilized ImageJ, a software program developed by the National Institutes of Health, to measure lattice constants. For example, Kobayashi et al. [22] calculated the rotation angles of Si (220) spacings using ImageJ ver. 1.52a and the fast Fourier transform pattern of the original TEM images. The TEM image was rotated according to the calculated angles so that the (220) spacings were perpendicular to the x -axis. Then, using a method similar to that of DigitalMicrograph, ImageJ measured the silicon lattice spacings. Therefore, irrespective of the kind of measurement software utilized, the manual operation method greatly relies on the experience of engineers and will introduce measurement errors; for example, engineers need to determine if the pulled rectangular frame is perpendicular to the measured lattice spacings and if the left and right sides of the dotted box are in the center of the lattice stripes. Furthermore, the more detailed process is complex, which makes it difficult to evaluate the reasonableness of the measurement results.

Therefore, to improve the measurement repeatability and accuracy of silicon lattice spacings in practical applications, this paper presents an automatic measurement method based on two-dimensional discrete Fourier transform (2D-DFT) and two-dimensional inverse discrete Fourier transform (2D-IDFT). Section 2 introduces the automatic measurement algorithm of the lattice spacings. Section 3 presents the experimental investigations. Finally, Sect. 4 presents the conclusions.

2 Measurement of Silicon Lattice Spacings

2.1 Measurement Principle

Two-dimensional DFT is a digital transformation method essential in numerous applications, such as image enhancement, denoising, edge detection, compression, and feature extraction. Moreover, it is a major technique in TEM application. For example, we can obtain diffraction-like patterns by performing 2D-DFT on an original TEM image, which is a concise and effective method if the sample size and the limitation of the selected area aperture hinder the acquisition of the diffraction pattern. In this paper, we propose a new silicon lattice spacing measurement approach based on the diffraction-like pattern.

After obtaining an HRTEM image, we perform 2D-DFT on the image containing the silicon lattice spacings. The original TEM image is denoted as $f(x, y)$; the transformed image is $F(u, v) = R_1(u, v) + i \times R_2(u, v)$, and its amplitude spectrum is

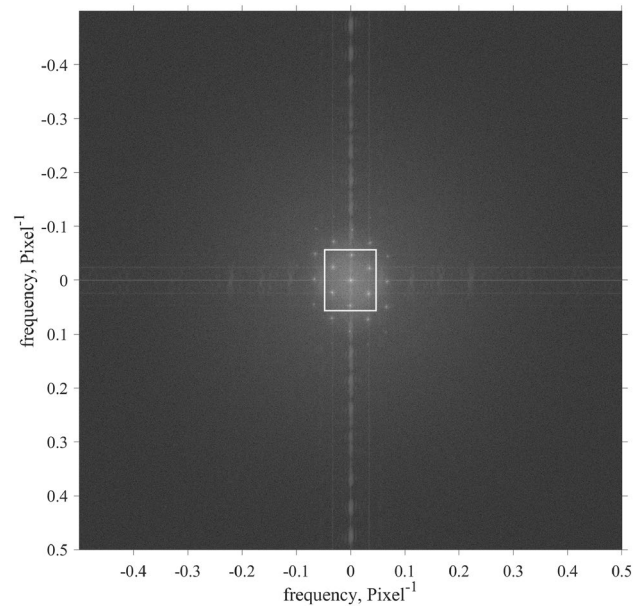


Fig. 3 2D-DFT pattern of the HRTEM image shown in Fig. 2

$$A(u, v) = \ln \left(\sqrt{R_1^2(u, v) + R_2^2(u, v)} \right) \quad (1)$$

where (x, y) and (u, v) denote the coordinates of the original image in the spatial and frequency domains, respectively, and the corresponding units are pixel and pixel^{-1} , respectively. Figure 3 shows the 2D-DFT pattern of the HRTEM image of Si shown in Fig. 2. Its zero-frequency component is shifted to the center of the spectrum.

According to the electron diffraction theory, one diffraction spot corresponds to a set of crystal lattice spacings. Therefore, we can obtain an image containing only a set of lattice spacings through 2D-IDFT for the central spot and a pair of diffraction spots. Then, we can accurately measure the lattice spacing through the gravity centre method after performing erosion and binarization operations on the image.

2.2 Bright Spot Extraction

To obtain an image containing only a set of lattice spacings after 2D-IDFT, we first need to extract the corresponding frequency components from the frequency domain image, that is, the bright spots symmetrical around the central bright spot. Each bright spot in the 2D-DFT image consists of multiple points.

We use the global threshold method to segment the spots from the amplitude spectrum image $A(u, v)$:

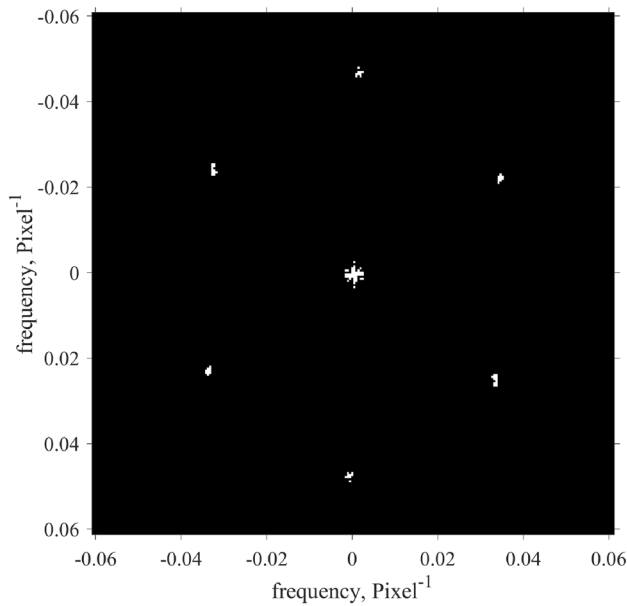


Fig. 4 Zoom-in view of the segmentation result of the marked area in Fig. 3

$$A'(u, v) = \begin{cases} 0, & \text{if } A(u, v) \leq T_1 \\ 1, & \text{if } A(u, v) > T_1 \end{cases} \quad (2)$$

where T_1 is the threshold, and its value is evaluated through statistical analysis of the grayscale value of the bright spots in the 2D-DFT pattern. Figure 4 shows a zoom-in view of the segmentation result of the marked area in Fig. 3 at $T_1 = 10$.

The distance between points in the same spot is much less than that between points in different spots. Therefore, we can extract the spots by scanning the points that meet this distance condition in the segmented image $A'(u, v)$. The extracted spots are shown in Fig. 5, in which points of the same color belong to the same spot. The number of points contained in each extracted bright spot is shown in Fig. 6. Under the same threshold segmentation condition, the central spot is greater than the other bright spots; that is, the extracted central spot contains more points than the others. Hence, the central spot can be identified from the extracted bright spots according to the maximum number of points.

2.3 Lattice Spacing Extraction and Measurement

After extracting the bright spots and identifying the central bright spot, we fit the central spot to the surrounding two symmetrical bright spots in a straight line “ $v = ku + b$.” The real part $R_1(u, v)$ and imaginary part $R_2(u, v)$ of $F(u, v)$ are processed as follows:

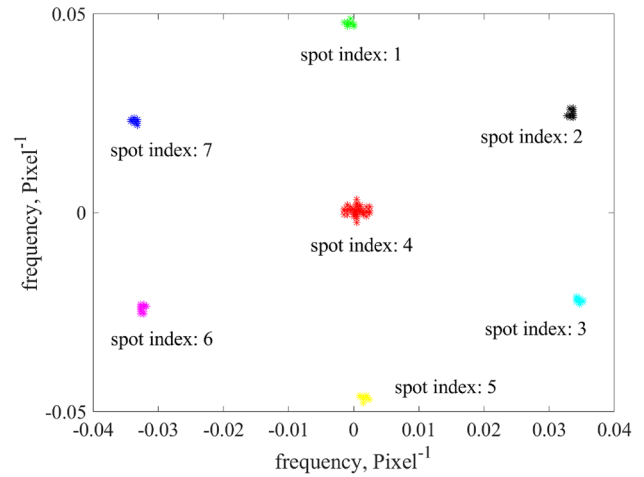


Fig. 5 Extracted spots based on distance; points of the same color belong to the same spot

$$R'_1(u, v) = \begin{cases} 0, & d = \frac{|ku - v + b|}{\sqrt{k^2 + 1}} \geq T_d \\ R_1(u, v), & d = \frac{|ku - v + b|}{\sqrt{k^2 + 1}} < T_d \end{cases} \quad (3)$$

$$R'_2(u, v) = \begin{cases} 0, & d = \frac{|ku - v + b|}{\sqrt{k^2 + 1}} \geq T_d \\ R_2(u, v), & d = \frac{|ku - v + b|}{\sqrt{k^2 + 1}} < T_d \end{cases} \quad (4)$$

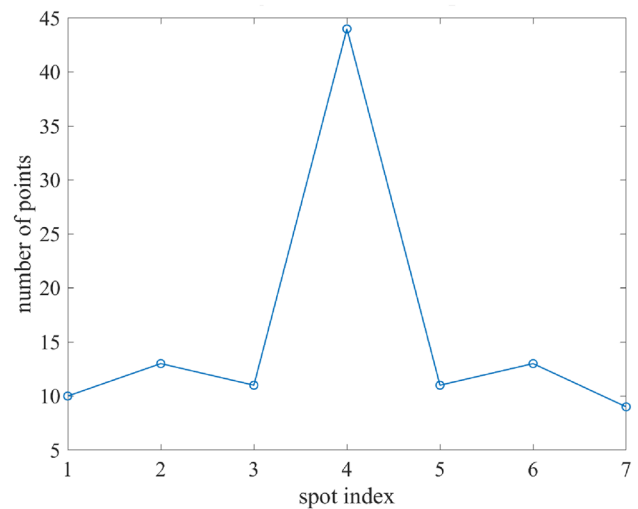


Fig. 6 Number of points contained in each extracted bright spot

where T_d denotes the threshold to constrain the normal width of the fitted straight line. T_d is 1.5 and is an empirical value. We can obtain a new transformed image $F'(u, v)$ as follows:

$$F'(u, v) = R'_1(u, v) + i \times R'_2(u, v) \tag{5}$$

After performing 2D-IDFT on $F'(u, v)$, we can obtain the image $f'(x, y)$, including a set of parallel lattice spacings (Fig. 7).

Owing to the uneven brightness of the image, we extract the local lattice spacing area, in which we perform morphological erosion and binarization. Because the line “ $v = ku + b$ ” is perpendicular to this group of parallel lattice spacings, the image $f'(x, y)$ can be rotated according to the slope k . The rotation angle is given as

$$\theta = \arctan\left(-\frac{1}{k}\right) \tag{6}$$

Figure 8 shows the extraction process of lattice spacings. From the intensity profile, we can accurately calculate the lattice spacing through the gravity centre method [23–25]. We obtain the threshold line using a configurable percentage of 75%, which denotes the distance between the threshold line and the top line. The top and bottom lines take the maximum and minimum positions of the intensity profile, respectively. The centre and peak positions are calculated inside the area surrounded by the threshold line and the intensity profile. Finally, the lattice spacing is calculated by the distance between two adjacent centres of gravity calculated in parallel with the threshold line. Figure 9 shows the measurement results of the gravity centre

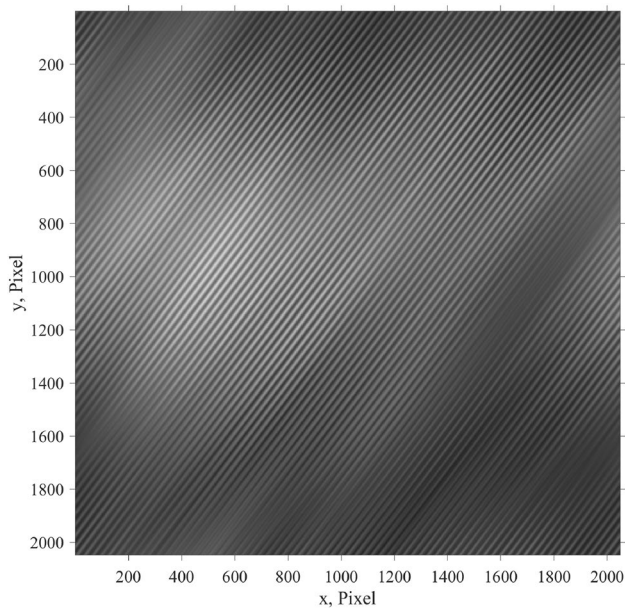


Fig. 7 An extracted set of parallel lattice spacings

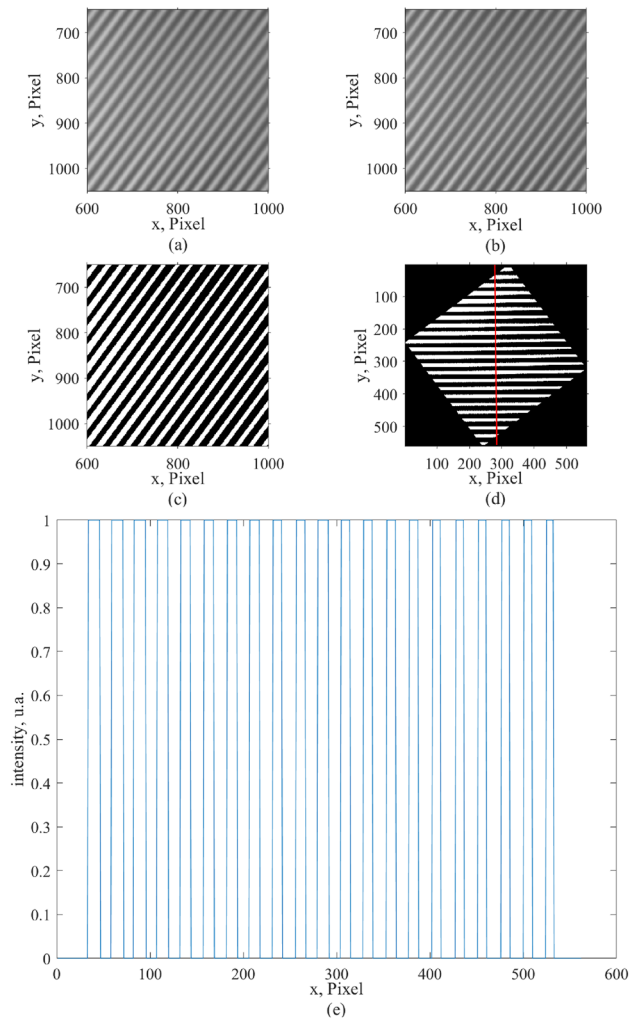


Fig. 8 Lattice spacing extraction process: a original image; b erosion operation; c binarization operation; d rotation operation; e intensity profile of the marked area in (d)

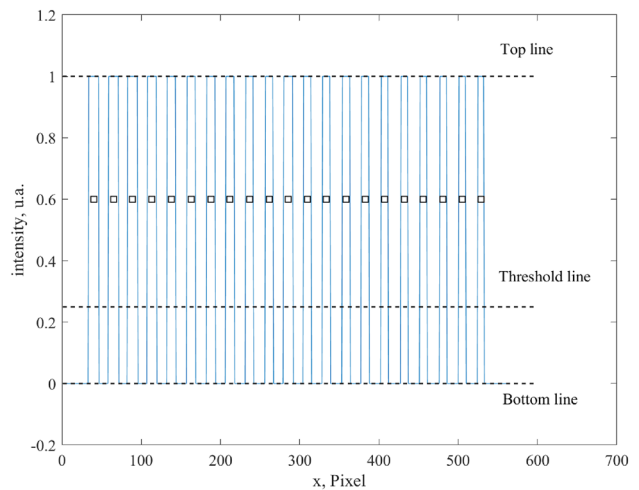


Fig. 9 Measurement results of the gravity centre method; “□” represents the gravity centre

method. There are 20 periodic crystal lattice spacings, and the total pixel span is 485.50. Hence, the pixel span of lattice spacing d_{111} is 24.28.

Multiple sets of symmetrical bright spots exist around the central spot; therefore, we can obtain multiple fitted straight lines. As shown in Fig. 5, three fitted straight lines correspond to the combination of bright spots as follows: {1, 4, 5}, {2, 4, 6}, and {3, 4, 7}. Therefore, three silicon lattice pixel spans will be produced after a series of processes. To improve the CD measurement accuracy, we calculate the estimated value of each lattice spacing according to the pixel size of the original TEM image, compare the values with the theoretical values from the standard powder diffraction file, and select the pixel span corresponding to the lattice spacing with the smallest error. The selected pixel span is used for CD estimation.

3 Experimental Investigations

We compared the proposed method with the DigitalMicrograph-based Si lattice spacing measurement method and applied the method for CD measurement.

3.1 Si lattice Spacing Measurement

To verify the effectiveness of the proposed automatic measurement method, we acquired HRTEM images with different magnifications (285 k, 450 k, 590 k, 790 k) for the same sample. We measured the d_{111} pixel span in these HRTEM images using the proposed method and DigitalMicrograph. The proposed method is more stable than the

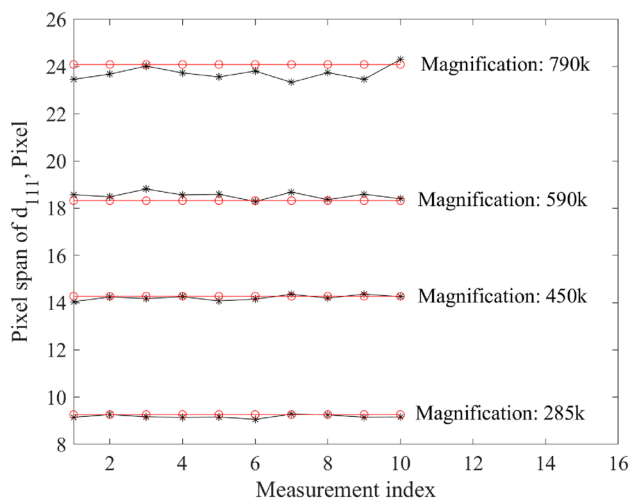


Fig. 10 Comparison of Si (111) lattice spacings obtained via the proposed method and the DigitalMicrograph-based method; “-o-” and “-*-*” represent the proposed method and DigitalMicrograph, respectively

DigitalMicrograph-based manual measurement method (Fig. 10).

3.2 Application in CD Measurement

The experimental sample was a nano line width with a nominal CD value of 22 nm. It was milled to a lamella by an ion beam thinner. The HRTEM image was acquired at the magnification of 450 k with 1024×1024 pixels (Fig. 11).

The averaged intensity profile of the marked area in Fig. 11 is shown in Fig. 12. The top and bottom intensities were manually measured on the material within the CD

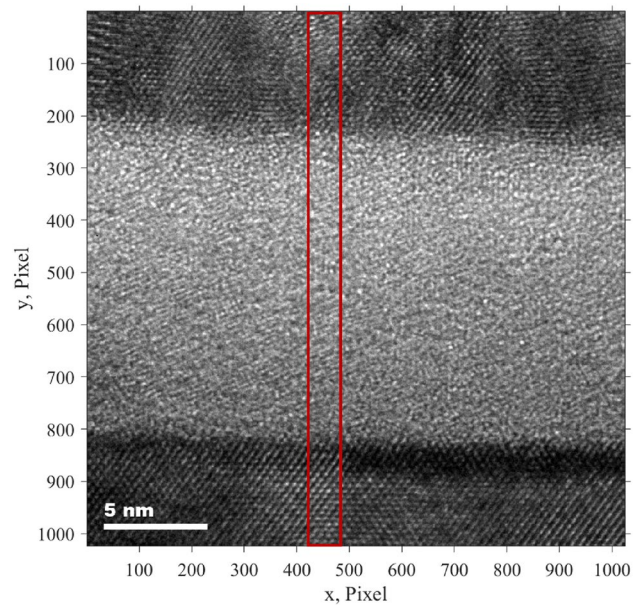


Fig. 11 Measured HRTEM image of line width

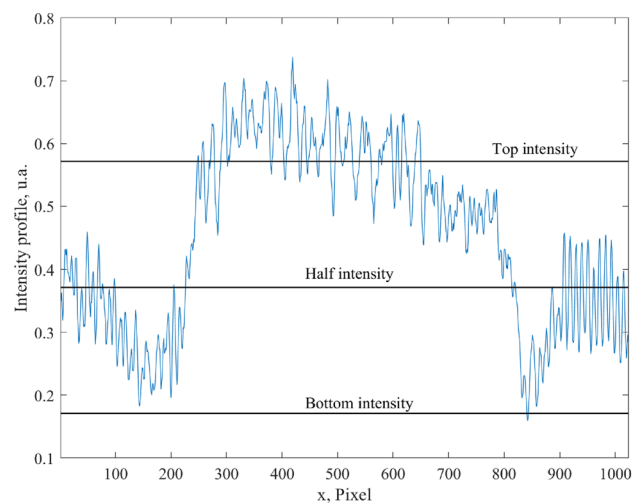


Fig. 12 Averaged intensity profile of the marked area in Fig. 11

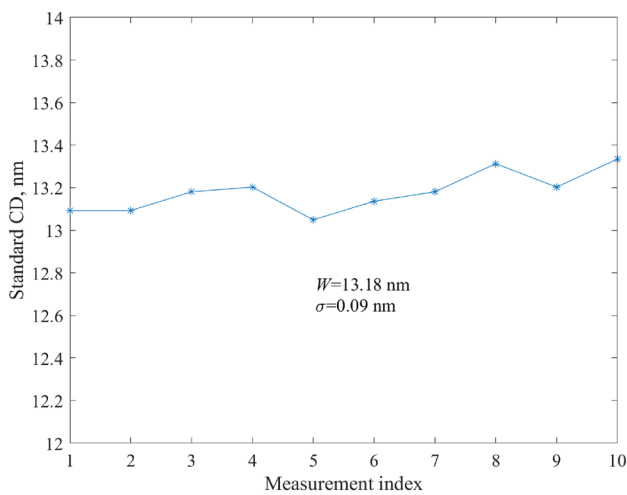


Fig. 13 Measurement results of the nano line width

structure and the silicon layer, respectively. The edge location of CD is defined at the half-intensity, which is determined by the top and bottom intensities.

The d_{111} pixel span was measured as 14.27 pixels using the proposed method. Ten CD measurements were conducted (Fig. 13). The standard deviation σ was 0.09 nm, and the average value (13.18 nm) was the standard CD of the line width.

4 Conclusions

This paper introduces an automatic 2D-DFT- and 2D-IDFT-based method for measuring Si lattice spacings in HRTEM images. We extract the spots from the diffraction image using the global threshold method. According to the electron diffraction theory, a set of lattice spacings is obtained through the 2D-IDFT of the central spot and a pair of diffraction spots. Afterward, the pixel span of the lattice spacing is calculated through the gravity centre method, and the standard CD value is estimated through the half-intensity method. Finally, using the proposed method, we measured a nano line width with a nominal CD of 22 nm. The results showed that the standard CD was 13.18 nm, and the standard deviation was 0.09 nm. The CD value is traceable to the SI meter definition by the lattice constant. Therefore, the proposed method can be applied for measuring nano line widths with atomic-level accuracy.

Some issues concerning the lattice spacing measurement require further research. In the future, we will investigate the impact of parameters T_1 and T_d on the measurement results. The lattice spacing (in the unit of a pixel) can also be directly calculated from the spectrum obtained using 2D-DFT. We will compare the lattice spacing with that obtained from the

proposed 2D-IDFT method. The locations of the top and bottom intensities and the physical meaning of the definition of half-intensity in HRTEM images also need to be studied.

Funding The project is supported by Basic Scientific Research Operating Fund of NIM (Grant No. AKYZD2007-1).

Declarations

Conflict of interest On behalf of all authors, the corresponding author states that there is no conflict of interest.

Open Access This article is licensed under a Creative Commons Attribution 4.0 International License, which permits use, sharing, adaptation, distribution and reproduction in any medium or format, as long as you give appropriate credit to the original author(s) and the source, provide a link to the Creative Commons licence, and indicate if changes were made. The images or other third party material in this article are included in the article's Creative Commons licence, unless indicated otherwise in a credit line to the material. If material is not included in the article's Creative Commons licence and your intended use is not permitted by statutory regulation or exceeds the permitted use, you will need to obtain permission directly from the copyright holder. To view a copy of this licence, visit <http://creativecommons.org/licenses/by/4.0/>.

References

1. Wu ZR, Cai YN, Wang XR, Zhang LF, Deng X, Cheng XB, Li TB (2019) Amorphous Si critical dimension structures with direct Si lattice calibration. *Chin Phys B* 28:030601
2. Hoefflinger B (2011) ITRS: the international technology roadmap for semiconductors, pp 161–174.
3. Habibullah H (2020) 30 years of atomic force microscopy: creep, hysteresis, cross-coupling, and vibration problems of piezoelectric tube scanners. *Measurement* 159:107776
4. Shi YS, Li W, Gao ST, Lu MZ, Hu XD (2018) Atomic force microscope scanning head with 3-dimensional orthogonal scanning to eliminate the curved coupling. *Ultramicroscopy* 190:77–80
5. Dai GL, Haßler-Grohne W, Huser D, Wolff H, Danzebrink H, Koenders L, Bosse H (2011) Development of a 3D-AFM for true 3D measurements of nanostructures. *Meas Sci Technol* 22:094009
6. Villarrubia JS (1997) Algorithms for scanned probe microscope image simulation, surface reconstruction, and tip estimation. *J Res Natl Inst Stan* 102:425–454
7. Dahlen G, Osborn M, Okulan N, Foreman W, Chand A, Foucher J (2005) Tip characterization and surface reconstruction of complex structures with critical dimension atomic force microscopy. *J Vac Sci Technol B* 23:2297–2303
8. Dai GL, Hahm K, Scholze F, Henn M, Gross H, Fluegge J, Bosse H (2014) Measurements of CD and sidewall profile of EUV photomask structures using CD-AFM and tilting-AFM. *Meas Sci Technol* 25:044002
9. Li YG, Zhang P, Ding ZJ (2013) Monte Carlo simulation of CD-SEM images for linewidth and critical dimension metrology. *Scanning* 35:127–139
10. Zhang P, Mao SF, Ding ZJ (2015) Monte Carlo study of the effective electron beam shape in scanning electron microscopic imaging. *Eur Phys J Appl Phys* 69:30703
11. Zou YB, Khan MSS, Li HM, Li YG, Li W, Gao ST, Liu LS, Ding ZJ (2018) Use of model-based library in critical dimension measurement by CD-SEM. *Measurement* 123:150–162

12. ISO/DIS 21466.1 (2019) Microbeam analysis - Scanning electron microscopy: method for evaluating critical dimensions by CD-SEM. International Organization for Standardization.
13. SI Brochure – 9th edition (2019) – Appendix 2. Mise en pratique for the definition of the meter in the SI, Consultative Committee for Length.
14. Yacoot A, Bosse H, Dixson R (2020) The lattice parameter of silicon: a secondary realisation of the metre. *Meas Sci Technol* 31:121001
15. Takamasu K, Kuwabara K, Takahashi S, Mizuno T, Kawada H (2010) Sub-nanometer calibration of CD-SEM line width by using STEM. *Metrol Insp Process Control Microlithogr XXIV* 7638:76381K
16. Orji NG, Dixson RG, Garcia-Gutierrez DI, Bunday BD, Bishop M, Cresswell MW, Allen RA, Allgair JA (2007) TEM calibration methods for critical dimension standards. *Metrol Insp Process Control Microlithogr XXI* 6518:651810
17. Dai GL, Heidelmann M, Kübel C, Prang R, Fluegge J, Bosse H, (2013) Reference nano-dimensional metrology by scanning transmission electron microscopy. *Meas Sci Technol* 24:085001
18. Dai GL, Fan Z, Heidelmann M, Fritz G, Bayer T, Kalt S, Fluegge J (2015) Development and characterisation of a new line width reference material. *Meas Sci Technol* 26:115006
19. Takamasu K, Okitou H, Takahashi S, Konno M, Inoue O, Kawada H (2012) Sub-nanometer calibration of line width measurement and line edge detection by using STEM and sectional SEM. *Proc SPIE* 8324:83240X 1–7
20. Takamasu K, Okitou H, Takahashi S, Konno M, Inoue O, Kawada H (2011). Sub-nanometer line width and line profile measurement for CD-SEM calibration by using STEM. *Proc SPIE*; 7971:797108 1–8.
21. Dai GL, Hahm K, Bosseand H, Dixson RG (2017) Comparison of line width calibration using critical dimension atomic force microscopes between PTB and NIST. *Meas Sci Technol* 28:065010
22. Kobayashi K, Misumi I, Yamamoto K (2021) Experimental evaluation of uncertainty in sub-nanometer metrology using transmission electron microscopy due to magnification variation. *Meas Sci Technol* 32:095011
23. Meli F, Thalmann R (1998) Long-range AFM profiler used for accurate pitch measurements. *Meas Sci Technol* 9:1087–1092
24. Misumi I, Gonda S, Kurosawa T, Takamasu K (2003) Uncertainty in pitch measurements of one-dimensional grating standards using a nanometrological atomic force microscope. *Meas Sci Technol* 14:463–471
25. Dai GL, Koenders L, Pohlenz F, Dziomba T, Danzebrink H (2005) Accurate and traceable calibration of one-dimensional gratings. *Meas Sci Technol* 16:1241–1249



Yushu Shi is an associate researcher at the National Institute of Metrology, China. And he is currently the director of the Nano Metrology Research Office and the leader of the innovation team in the field of micro-nano metrology. He has focused on the needs of the micro-nano industry, closely followed the development of cutting-edge technologies at home and abroad, broke through several key technical bottlenecks, and carried out much fruitful work.